

acknowledges the receipt of the James Franck fellowship. This work was supported by the National Science Foundation-Materials Research Laboratory Grants No. DMR-78-11771 and No. DMR-79-23573, and by the U. S. Department of Energy.

<sup>(a)</sup>Permanent address: Institute of Physics, Beijing, People's Republic of China.

<sup>(b)</sup>Permanent address: Department of Physics and Astronomy and Materials Research Center, Northwestern University, Evanston, Ill. 60201 and Argonne National Laboratory, Argonne, Ill. 60439.

<sup>1</sup>P. G. deGennes, *J. Phys. (Paris)*, Colloq. **30**, C4-65 (1969).

<sup>2</sup>P. C. Martin, O. Parodi, and P. S. Pershan, *Phys. Rev. A* **6**, 2401 (1972).

<sup>3</sup>K. Miyano and J. B. Ketterson, *Physical Acoustics*

(Academic, New York, 1979), Vol. XIV, p. 93.

<sup>4</sup>York Liao, Noel A. Clark, and P. S. Pershan, *Phys. Rev. Lett.* **30**, 639 (1973).

<sup>5</sup>M. Liu, *Phys. Rev. A* **19**, 2090 (1979).

<sup>6</sup>N. A. Clark, *Phys. Rev. A* **14**, 1551 (1976); R. Ribotta, *C. R. Acad. Sci., Ser. B* **279**, 295 (1974); H. Birecki, R. Schaetzing, F. Rondelez, and J. D. Litster, *Phys. Rev. Lett.* **36**, 1376 (1979).

<sup>7</sup>L. Richard and J. Prost, *J. Phys. (Paris)*, Colloq. **40**, C3-83 (1979).

<sup>8</sup>M. R. Risch, L. B. Sorensen, and P. S. Pershan, to be published.

<sup>9</sup>Y. Kawamura and S. Iwayanagi, in *Proceedings of the Eighth International Liquid Crystal Conference*, Kyoto, 1980 (to be published).

<sup>10</sup>K. Miyano and J. B. Ketterson, *Phys. Rev. Lett.* **31**, 1047 (1973).

<sup>11</sup>B. Y. Cheng, Bimal K. Sarma, S. Bhattacharya, and J. B. Ketterson, to be published.

<sup>12</sup>D. Forster, T. C. Lubensky, P. C. Martin, J. Swift, and P. S. Pershan, *Phys. Rev. Lett.* **26**, 1016 (1971).

<sup>13</sup>K. Miyano, private communication.

## Determination of Internal-State Distributions of Surface Scattered Molecules: Incomplete Rotational Accommodation of NO on Ag(111)

Gary M. McClelland,<sup>(a)</sup> Glenn D. Kubiak, Harry G. Rennagel, and Richard N. Zare  
*Department of Chemistry, Stanford University, Stanford, California 94305*

(Received 29 December 1980)

Laser-induced fluorescence has been used to measure the rotational-state distribution of nitric oxide scattered from clean, single-crystal silver. Each resulting distribution is described by a rotational temperature within the statistical uncertainty. As the surface temperature is increased from 475 to 615 to 720 K, the calculated rotational temperature varies from  $360 \pm 50$  to  $430 \pm 90$  to  $405 \pm 60$  K, respectively. This shows that not only is rotational accommodation incomplete, but the degree of accommodation may decrease at the highest surface temperature studied.

PACS numbers: 68.45.-v, 79.20.Nc, 82.65.My

We report the determination of the rotational-state distribution of scattered nitric oxide molecules when an uncollimated room-temperature effusive beam of NO strikes a well characterized Ag(111) surface maintained at various temperatures. For each surface temperature studied in the range between 475 and 720 K, the scattered molecular rotational state distributions are well represented by Maxwell-Boltzmann distributions corresponding to rotational temperatures,  $T_R$ , which are 100 to 300 K less than the surface temperature,  $T_S$ . In the current experiments the state determinations are made in a manner that integrates over both scattering angle and velocity.

Although the body of experimental gas-surface scattering data is growing rapidly, nearly all in-

formation obtained to date concerns the angular and velocity distributions of the scattered particles.<sup>1,2</sup> For monatomic gases this represents sufficient information to test available dynamical theories<sup>3</sup> and eventually to estimate the potential energy surfaces governing the dynamics. For molecular gases, however, additional information is required, namely, the specification of the populations of internal states of the scattered species. The internal-state distributions of surface-scattered<sup>4</sup> and desorbed<sup>5</sup> N<sub>2</sub> have been determined previously by electron-impact fluorescence. However, when laser-induced fluorescence<sup>6</sup> is applicable, this technique should prove superior. Laser-induced fluorescence has been applied to the measurement of the velocity distribution of sput-

tered sodium atoms,<sup>7</sup> to the detection of OH molecules from an uncharacterized platinum surface,<sup>8</sup> and to the determination of the internal-state distributions of CO molecules scattered from LiF,<sup>9</sup> and NO molecules scattered from both graphite covered and nitric oxide covered platinum.<sup>10</sup>

The apparatus employed in the present study, shown schematically in Fig. 1, is a two-tiered, stainless steel ultrahigh-vacuum chamber having a base pressure of  $2.0 \times 10^{-10}$  Torr. The sample is transported from the surface analysis to the scattering and fluorescence regions by a magnetically coupled linear motion manipulator. Nitric oxide effused from a stainless steel capillary 0.3 cm from the surface was scattered from the surface, and was excited by an ultraviolet light beam passing 0.7 cm from the surface, where no excitation of the incident NO can occur. The relative population of the rotational states was deduced from the excitation wavelength dependence of the total undispersed fluorescence intensity detected by a solar blind photomultiplier.

The sample surface was prepared from a 12.7 mm diameter, 1.9 mm thick disk which had been

oriented to within  $1^\circ$  of the (111) plane (Monocrystals Co., 99.999% pure). The sample was mechanically polished by standard metallurgical methods and then chemically polished with a dilute solution of KCN and  $H_2O_2$ .<sup>11</sup> The crystal is mounted on the end of a tantalum cylinder containing a tungsten ribbon for radiative heating. *In situ* ion bombardment cleaning reduced the surface concentrations of all contaminants except sulphur to below the minimum detection sensitivity ( $<1\%$ ) of the retarding field analysis Auger electron spectrometer when used in conjunction with the grazing incidence electron gun. Repetitive ion bombardment ( $E_{Ar^+} = 300$  eV,  $I_{Ar^+} = 7.5 \times 10^{-7}$  A/cm<sup>2</sup>) was employed until the S(152 eV)/Ag(351, 356 eV) peak ratio ceased to change from its minimum value of  $8.0 \times 10^{-3}$ . Sample annealing was done by repetitively flashing to 800 K until a sharp ( $1 \times 1$ ) low-energy electron diffraction pattern was produced. This cleaning and annealing cycle was performed prior to and, when necessary, during data acquisition.

The flux of NO at the surface was estimated to be  $2.7 \times 10^{15}$  molecules/cm<sup>2</sup> sec ( $\sim 7$  monolayers/sec). The diffuse background NO pressure during each experiment was  $1.8 \times 10^{-8}$  Torr. When the chamber was filled with NO at a pressure that mimicked the experimental scattering flux, spectra from the Auger electron spectrometer disclosed the presence of nitrogen and oxygen only for  $T_s = 300$  K, but not for  $T_s = 475, 615, \text{ or } 720$  K. This is consistent with the facts that the saturation coverage and heat of adsorption of NO on Ag(111) are 0.05 and 103 kJ/mol, respectively.<sup>12</sup> If we assume  $\nu_{ad} = 10^{13}$ /sec for each adsorption site,<sup>12</sup> the desorption rate is approximately 50/sec per site, even at 475 K.

Ultraviolet light used to excite the (1,0) band of the NO A-X system at 2145–2155 Å was produced by focusing the tunable 5778–5700 Å output of a Nd-doped yttrium-aluminum-garnet-pumped dye laser into a high-pressure H<sub>2</sub> cell to give seventh-order anti-Stokes stimulated Raman emission. The measured bandwidth and energy were  $1.1 \text{ cm}^{-1}$  and  $12 \mu\text{J/pulse}$ , respectively.

To correct for both random and wavelength-dependent intensity fluctuations, we simultaneously recorded the NO fluorescence spectra from the surface-scattered molecules and from a room-temperature bulb (reference cell) containing NO at a pressure of 10 mTorr. Both photomultiplier photocurrents were processed by a gated integrator and stored in a signal averager. The simultaneously recorded spectra allow us to determine

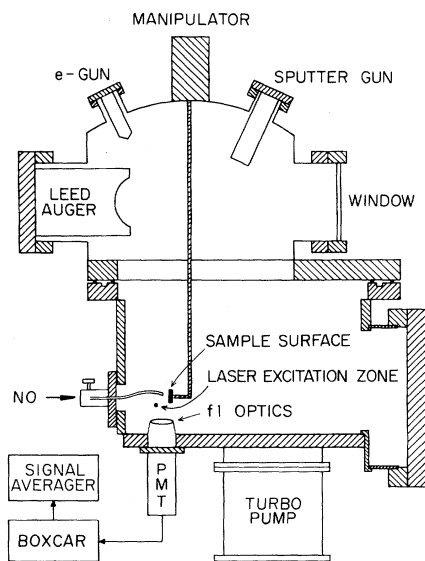


FIG. 1. Schematic cross section of the surface analysis and scattering apparatus. The upper surface analysis region includes a retarding field analysis Auger electron spectrometer, grazing incidence electron gun, low-energy electron diffraction optics, and Ar<sup>+</sup> sputtering gun. The lower surface scattering region contains a simple capillary effusive source, laser entrance port, and beam dump.

the intensity ratio,  $\mathcal{g}$ , defined as

$$g = \frac{I_{\text{scat}}}{I_{\text{ref}}}, \quad (1)$$

where  $I_{\text{scat}}$  and  $I_{\text{ref}}$  are the intensities of the surface-scattered and reference spectrum, respectively, at a given feature.

Typically, eight surface-scattered spectra were averaged in a process that required approximately one hour. Figure 2 shows the resulting excitation spectra recorded for NO scattering from (a) 720 K Ag(111), and (b) 690 K rough, oxidized stainless steel, which is expected to fully accommodate incident molecules. It should be noted that 20% of the signal intensity shown in Fig. 2 originates from background NO. This is ascertained from the spectra taken after the sample is withdrawn from the scattering and fluorescence collection region. All subsequent discussion will concern spectra for which this background has been subtracted.

We quantitatively express the information contained in the spectra such as those shown in Fig. 2 in two ways. The first is to determine the ratio,  $\epsilon$ , of the integrated intensities of the band-

heads labeled  $P_2$  and  $P_{12}$  in Fig. 2:

$$\epsilon(T_R) = \frac{[\mathcal{g}_{P_{12}, \text{scat}} - \mathcal{g}_{P_{12}, \text{bkngd}}]}{[\mathcal{g}_{P_2, \text{scat}} - \mathcal{g}_{P_2, \text{bkngd}}]}. \quad (2)$$

The subscripts *scat* and *bkngd* refer to surface-scattered and background (surface withdrawn) values, respectively, and the intensities  $\mathcal{g}$  are as defined in Eq. (1).  $\epsilon(T_R)$  is an increasing function of the rotational temperature because the rotational quantum numbers ( $N''$ ) of the spectral lines forming the  $P_{12}$  bandhead are generally eight higher than those of the lines forming the  $P_2$  bandhead (see Fig. 2).

The functional dependence of  $\epsilon$  on  $T_R$  was determined by computer simulation by using known rotational line strengths,<sup>13</sup> weighting by the appropriate Boltzmann factors, and convoluting with the laser bandwidth. The rotational temperatures obtained from the values of  $\epsilon$  by this inversion procedure are plotted in Fig. 3. It is apparent from Fig. 3 that the rotational temperature determined from the Ag-scattered NO is always less than the value expected for full rotational accommodation. It is also apparent that the value of  $T_R$  obtained from stainless-steel-scattered NO corresponds very closely to  $T_S$ , as would be expected.

We cannot measure directly relative populations of individual rotational states because each resolved spectral feature in the  ${}^2\Pi_{3/2}$  subband is composed of overlapping rotational lines from two

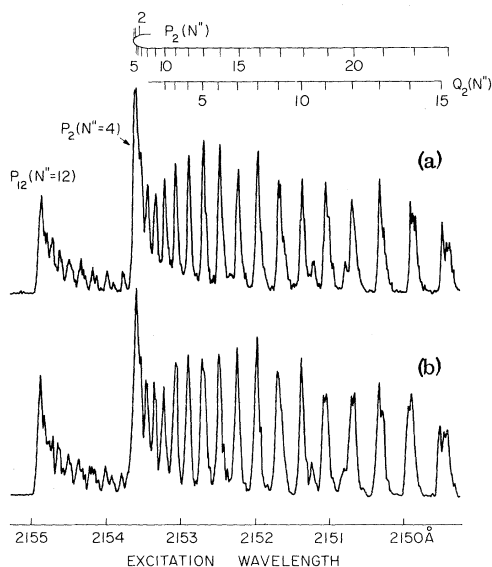


FIG. 2. The excitation spectra produced when the surface-scattered NO flux was intersected with the laser 0.7 cm from the crystal and 0.35 cm below and behind the capillary orifice: (a) Ag(111),  $T_S = 720$  K, and (b) rough, oxidized stainless steel,  $T_S = 690$  K. Estimated particle density is  $3.2 \times 10^9 \text{ cm}^{-3}$ .

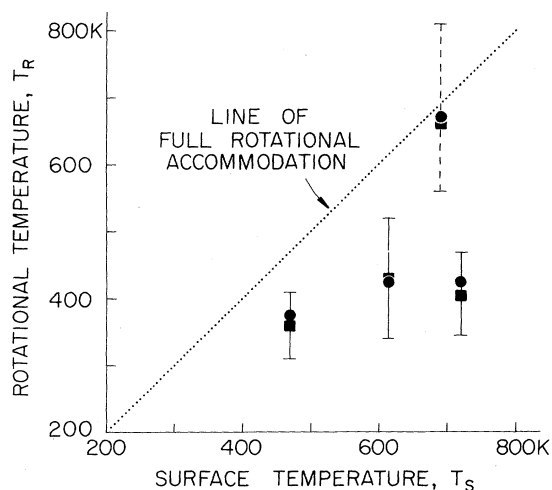


FIG. 3. Plot of  $T_R$  vs  $T_S$ : full squares obtained from bandhead ratios,  $\epsilon(T_R)$ , and full circles obtained from best fit to line features. The solid error bars refer to scattering of NO from Ag(111), the dashed error bar to stainless steel.

TABLE I. Summary of NO scattering conditions, rotational temperatures, and rotational accommodation coefficients. Uncertainties listed are one standard deviation.

Surface	$T_S$	$T_R^a$	$T_R^b$	$\gamma(T_R)^c$
Ag(111)	475 K	360 ± 50 K	375 ± 100 K	0.40 ± 0.33
Ag(111)	615 K	430 ± 90 K	425 ± 175 K	0.42 ± 0.29
Ag(111)	720 K	405 ± 60 K	425 ± 125 K	0.26 ± 0.15
Stainless steel	690 K	660 ± 110 K	670 ± 110 K	0.92 ± 0.28

<sup>a</sup>Determined from calculated dependence of  $\epsilon$  on  $T_R$ .

<sup>b</sup>Determined from best fit of calculated to experimental line intensities.

<sup>c</sup>The rotational accommodation coefficient  $\gamma$  is defined by  $\gamma(T_R) = (T_{inc} - T_R)/(T_{inc} - T_S)$ , where  $T_{inc}$  is the temperature of the incident beam.

neighboring branches having values of  $N''$  differing by eight. As an alternative we have compared the total integrated intensity of each resolvable feature in this subband with that simulated for a given temperature  $T_R$ . For every surface temperature studied, the best (least squares) fit to the observed line intensities yielded the result that  $T_R$  was much less than  $T_S$  (see Table I). The values of  $T_R$  determined by this method are in close agreement to those obtained by the procedure explained earlier, as shown in Fig. 3. The uncertainty is larger for those values of  $T_R$  derived from the computer simulation of the (blended) line intensity distributions because the latter are less sensitive to temperature change than the bandhead ratio.

We conclude that the rotational distributions measured for Ag(111)-scattered nitric oxide are adequately described by Maxwell-Boltzmann distributions and that the corresponding rotational temperatures show the rotational accommodation on this surface to be far from complete. Microscopic reversibility requires that molecules leaving the surface are at thermal equilibrium with the surface if the sticking coefficient for chemisorption is unity. However, for the NO/Ag(111) system the sticking coefficient is quite low ( $< 0.1$ ),<sup>12</sup> indicating the importance in addition to chemisorption of one or more of the scattering classifications of Weinberg and Merrill:<sup>14</sup> quasi-elastic, inelastic, and trapping followed by desorption. Characteristic angular and velocity distributions are associated with each of the above

four mechanisms, but our continuous uncollimated source of incident molecules averages over these characteristics. We are preparing experiments that will use a collimated pulsed nozzle beam which will provide the velocity, angle, and temporal resolution necessary to measure separately internal-state distributions following each of the four scattering processes.

We thank Sylvia Ceyer and Jonathan Sokol for advice on apparatus design, and Phillip C. McKernan for help with the sample holder. One of us (G. M. M.) thanks the National Science Foundation for a National Needs Postdoctoral Fellowship. This research was sponsored by the U. S. Office of Naval Research under Contract No. ONR-N00014-78-C-0403 and the U. S. Army Research Office under Contract No. ARO-DAAG-29-80-K-0035.

<sup>(a)</sup>Present address: Department of Chemistry, Harvard University, Cambridge, Mass. 02138.

<sup>1</sup>W. H. Weinberg, *Adv. Colloid Interface Sci.* **4**, 301 (1975).

<sup>2</sup>For an excellent review, see F. O. Goodman and H. Y. Wachman, *Dynamics of Gas-Surface Scattering* (Academic, New York, 1976).

<sup>3</sup>J. C. Tully, *Annu. Rev. Phys. Chem.* **31**, 319 (1980).

<sup>4</sup>V. Ramesh and D. J. Marsden, *Vacuum* **24**, 291 (1974).

<sup>5</sup>R. P. Thorman, D. Anderson, and S. L. Bernasek, *Phys. Rev. Lett.* **44**, 743 (1980).

<sup>6</sup>R. N. Zare and P. J. Dagdigian, *Science* **185**, 739 (1974).

<sup>7</sup>W. Husinsky and R. Bruckmuller, *Surf. Sci.* **80**, 637 (1979).

<sup>8</sup>D. E. Tevault, L. D. Talley, and M. C. Lin, *J. Chem. Phys.* **72**, 3314 (1980).

<sup>9</sup>J. C. Polanyi, private communication.

<sup>10</sup>F. Frenkel, J. Häger, W. Krieger, H. Walther, C. T. Campbell, G. Ertl, H. Kuipers, and J. Segner, *Phys. Rev. Lett.* **46**, 152 (1981).

<sup>11</sup>J. Morabito, R. Steiger, R. Muller, and G. A. Somorjai, in *Structure and Properties of Solid Surfaces*, edited by G. A. Somorjai (Wiley, New York, 1969), p. 50-51.

<sup>12</sup>P. J. Goddard, J. West, and R. M. Lambert, *Surf. Sci.* **71**, 447 (1978).

<sup>13</sup>Calculated from spectroscopic constants; see R. N. Zare, *Molecular Spectroscopy: Modern Research* (Academic, New York, 1972), p. 207.

<sup>14</sup>W. H. Weinberg and R. P. Merrill, *J. Chem. Phys.* **56**, 2881 (1972).